A study of coherent bremsstrahlung and radiative capture

Hoefman, Marieke

3. Setup and experimental facilities

In this chapter first the $\alpha + \mathrm{p}$ experiment and setup will be described. Also, a description of two general experimental facilities at the *KVI* will be given, with which the author was particularly involved: the *Carbon–Fibre Scattering Chamber* and the *Forward Wall*. The *Carbon–Fibre Scattering Chamber* was also part of the $\alpha + \mathrm{p}$ experiment. The *Forward Wall* has been used in heavy–ion bremsstrahlung experiments.

3.1 Setup of α+p experiment

In figure 3.1 the experimental setup for the $\alpha + \mathrm{p}$ experiment is shown. The geometry of this setup was predetermined by the experiments preceding and following this study. A 200 MeV α beam was delivered by the new *AGOR*[*] cyclotron of the *KVI*. The beam was incident on a liquid hydrogen target with a thickness of (56.3 ± 2.5) mg/cm^2. The foil windows of the target were made as thin as possible to minimize its contribution to the background. The target was placed in the *Carbon–Fibre Scattering Chamber*. The bremsstrahlung photons were measured by the Two–Arm Photon Spectrometer *TAPS*. *TAPS* was configured in 6 blocks of 64 BaF_2–detectors each. It covered an angular range between 57° and 176° and had a vertical acceptance of $\pm$ 23°. At forward angles the Small–Angle Large–Acceptance Detector *SALAD* was positioned. It consists of two wire chambers and two layers of scintillators and measures the position and energy of the outgoing particles. In the $\alpha + \mathrm{p}$ experiment typically one of the outgoing particles was measured by *SALAD*.

A more extended description of the liquid hydrogen target, *TAPS*, *SALAD*, the trigger logic and the *Carbon–Fibre Scattering Chamber* can be found in sections 3.1.2, 3.1.3, 3.1.4, 3.1.5 and 3.2, respectively.

[*] Accélérateur Groningen–ORsay

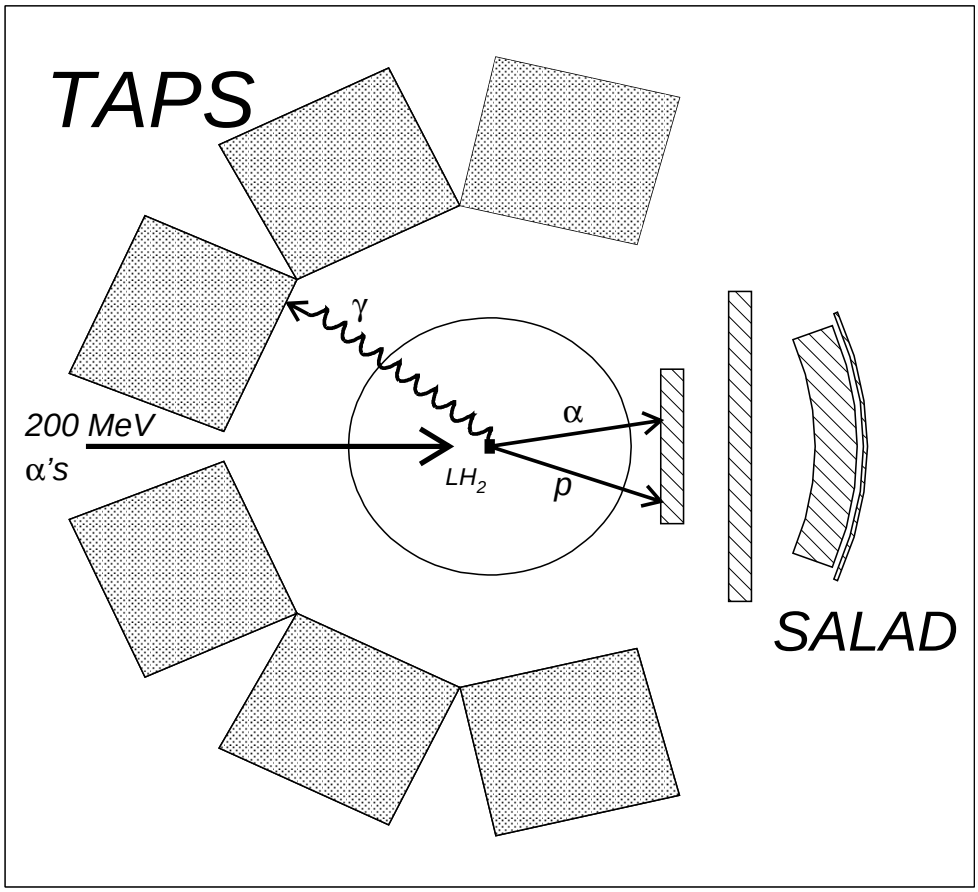

Figure 3.1: The *TAPS* + *SALAD* setup at *KVI*. The α beam enters at the left. It hits the liquid hydrogen target in the center of the *Carbon–Fibre Scattering Chamber*. The 6 *TAPS* blocks are shown, as well as *SALAD* at forward angles.

3.1.1 AGOR

AGOR is a cyclotron with superconducting coils [Sch98a, and references therein]. The cyclotron has been constructed at *IPN* in Orsay, in a collaboration between *IPN* and *KVI*. It has a bending limit of K = 600 MeV and can accelerate both protons and heavy ions. For protons, the maximum accelerated energy is 200 MeV, while for heavy ions, this energy depends on their charge–to–mass ratio q/A. For $q/A = 0.5$ the maximum energy is 95 MeV/nucleon.

In April 1994, the first test beam of α–particles of 200 MeV was extracted from *AGOR* at Orsay. After these tests, the cyclotron was disassembled and reassembled again at *KVI* in Groningen. In the fall of 1995 the same α–beam was accelerated again internally. Complete extraction of the beam was performed

in january 1996. In that same year, the first campaign of experiments with *AGOR* was scheduled, with the *TAPS* and *SALAD* setup. The α + p experiment, discussed in this thesis, was part of that campaign.

3.1.2 Liquid hydrogen target

The liquid hydrogen target [Zij95, Kal98a] has been designed especially for the few–body studies at *KVI*. It has a diameter of 20 mm and a thickness of 6 mm. The aluminium frame around the target has a width of 5 mm. Thin foil windows are mounted at the front and at the back of the target hole. For 10 and 100 MeV photons, which are emitted in the direction of the target frame, a maximum of 1.5 and 5 % will be absorbed, respectively, depending on the distance traveled through the aluminium.

After filling with liquid hydrogen, the target thickness will be larger than the nominal 6 mm, due to the bulging of the target in the middle. The average thickness of the target of (56.3 ± 2.5) mg/cm^2 was determined from the elastic proton scattering obtained during the p + p bremsstrahlung experiment [Hui99a], using the known elastic scattering cross sections. The quoted error reflects the accuracy, with which the elastic pp cross section could be measured. In particular, it depends on the mean variation in target thickness over a period of several days and the charge collection efficiency of the Faraday cup, which is assumed to be 100 %. In fact, the efficiency of the Faraday cup is indeed close to 100 % for both protons and α–particles. However, there might be variations due to the beam quality, having an effect in the order of 10 % for protons and slightly less for α–particles [Sch98]. Unfortunately, the precise conditions and, more importantly, its effects on the Faraday cup during the α + p experiment are not known, but assumed to be not worse due to the lower energy and higher charge of the α–beam, with respect to the proton beam.

Foil windows of synthetic material have been selected after testing under various conditions [Kal98a]. The windows used were made of Aramid[†] and were

[†] called TX-I, from Toray, Japan

element	weight	atomic
N	9%	7%
C	57%	50%
H	3%	31%
O	11%	7%
Cl	21%	6%

Table 3.1: Composition of the Aramid foils.

very thin: 0.55 mg/cm^2. The composition of these foils is listed in table 3.1. By way of precaution they were replaced after each experiment. The target was placed in the *Carbon–Fibre Scattering Chamber* (section 3.2) and 'wobbled' constantly over a distance of 2 mm to assure a homogenous target and to prevent localized radiation damage in the target windows.

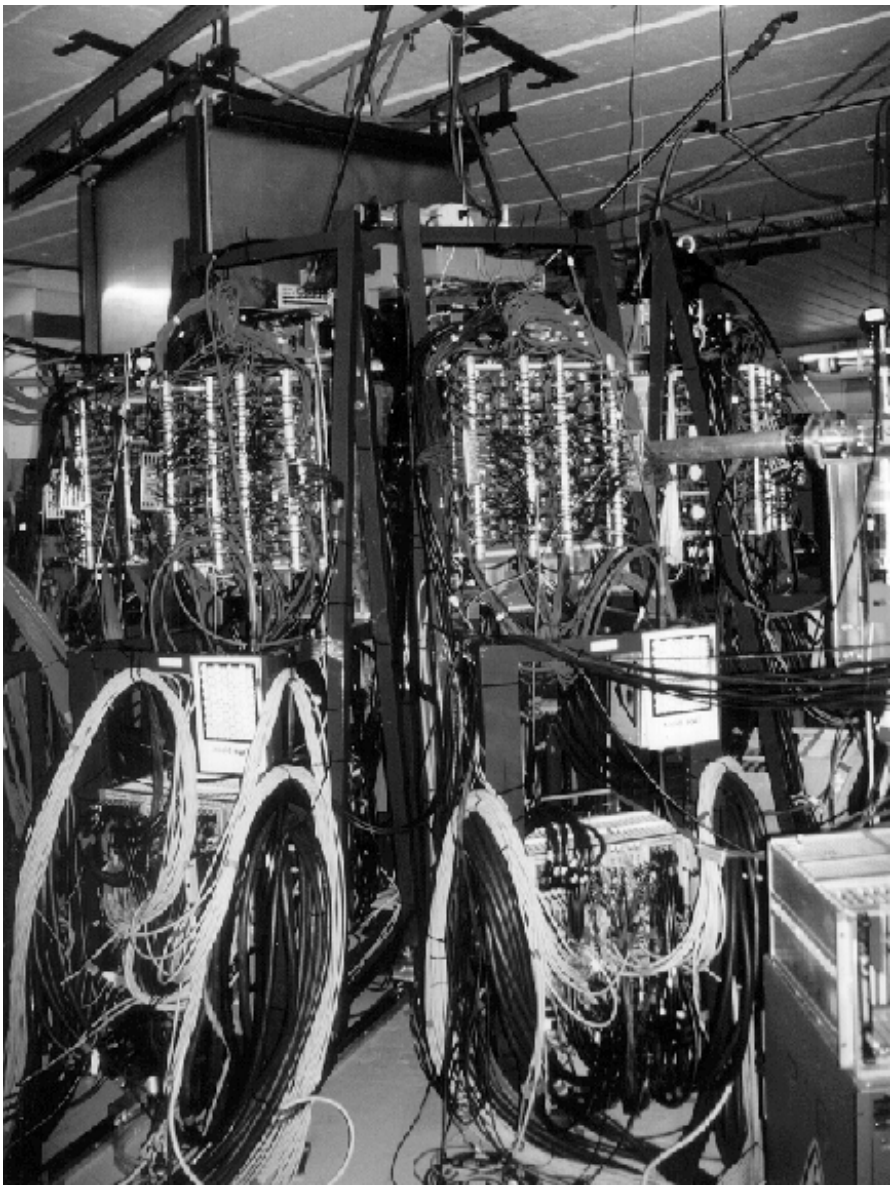

Figure 3.2: Photo of the $\alpha + p$ setup. The α beam enters at the right and the backside of two of the *TAPS* blocks can be seen.

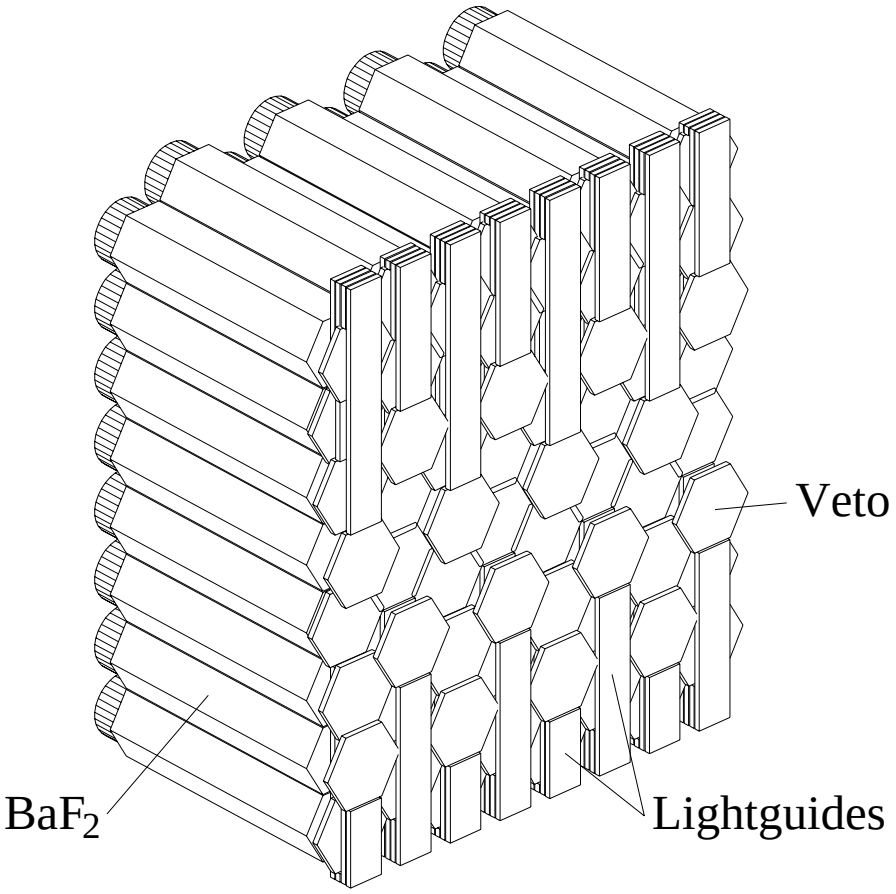

Figure 3.3: One *TAPS*–block with 64 BaF_2–cristals and 64 veto–detectors.

3.1.3 TAPS

In the $\alpha + p$ experiment the 'Two–Arm Photon Spectrometer' *TAPS* [Str96, Mar95, Gab94, Nov91] was configured in 6 blocks of 64 BaF_2 crystals each. The blocks were positioned at a distance of 66 cm from the target at -76.5°, -116.5°, -156.5°, 156.5°, 116.5° and 76.5° with respect to the beam direction (see figure 3.1). Part of the actual setup can be seen in figure 3.2, where two of the *TAPS*–blocks are seen from the backside.

3.1.3.1 TAPS detector

In figure 3.3, the configuration of one *TAPS*–block is shown. There are 64 BaF_2 crystals in each block. Each crystal has a charged–particle veto detector in front. In this $\alpha + p$ experiment the *TAPS*–blocks were used in a position where the housing of the photomultipliers of the charged–particle vetos is on the top and

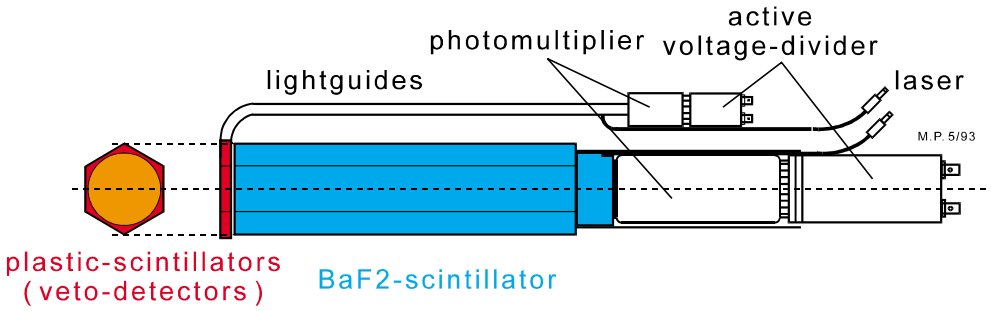

Figure 3.4: A *TAPS*–detector with a veto–detector in front.

bottom of the *TAPS*–block (see figure 3.3). This configuration reduces the 'dead' areas between two adjacent *TAPS*–blocks and results in a maximal coverage in polar angle, only restricted in the forward angles by the mounting structures of *SALAD*.

In figure 3.4, one of the BaF_2 modules is shown. Each crystal is hexagonally shaped with a length of 25 cm. The inner part of the hexagon has a diameter of 5.9 cm.

The BaF_2 crystals have a light output consisting of a fast (τ=0.6 ns) and a slow (τ=620 ns) component. The fast component is quenched with increasing dE/dx, resulting in a pulse shape which allows to distinguish between hadronic and electromagnetic particles (see subsection 4.1.1.3). The timing properties of the crystals are extremely good (85 ps), which can be used to distinguish between photons and neutrons using the time–of–flight of these particles. In the α + p experiment, the timing properties were limited by the time–width of the α–beam, as discussed in subsection 4.1.1.1. However, this broad width of about 2 ns did not influence the good separation between neutrons and photons, since at these energies, the time–of–flight of neutrons is quite long.

To select charged from non–charged particles a charged–particle veto detector (CPV) is placed in front of each BaF_2 detector. This CPV has the same hexagonal shape as the BaF_2 detector. It is made of scintillating plastic (NE102A) and has a thickness of 5 mm. A light guide transports the signal to the photomultipliers at the top and bottom of each *TAPS*–block.

3.1.3.2 TAPS electronics

For the analysis, the deposited energies of all BaF_2 crystals have to be read out. The collected charge is integrated in a wide and a narrow gate, resulting in the total energy (E_{wide}) as well as ΔE (E_{narrow}), respectively. The latter is needed to obtain the pulse shape information. Also, the time–of–flight signals of the BaF_2 crystals have to be known, as well as the threshold information, which is used to

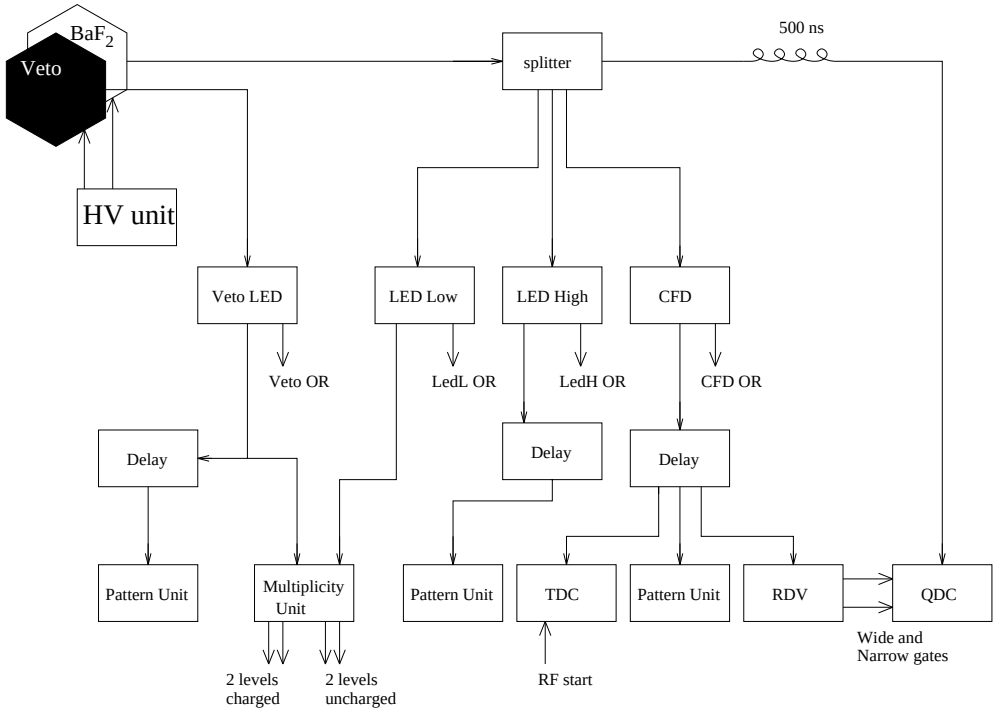

Figure 3.5: *TAPS* electronics scheme.

build the trigger and for the decision about the importance of the event. For the CPV detectors, only the threshold information is used, to decide whether or not the detected particle was charged.

The *TAPS*–electronics scheme for each BaF_2 crystal and CPV is drawn in figure 3.5. The signal of the BaF_2 crystal is split into 4 outputs. The analog output is delayed and integrated in the QDC. The other 3 signals are used for gating (CFD) and trigger information (LED)[‡]. The signal from the veto was only used for trigger information. The two LED thresholds for the BaF_2 detectors are set at different levels. The highest level (LED High) was set at 10 MeV and the lowest level (LED Low) at 5 MeV, except for the two most forward blocks (see fig 3.1). To decrease the trigger rate for these, their LED Low thresholds were set at 7 MeV. The thresholds can be set individually for each detector. The CFD threshold was as low as possible, which was about 0.4 MeV.

As mentioned, the analog signal of the BaF_2 detector is integrated in the QDC and the RDV supplies the two gates (long and short) to the QDC. The time is measured with the TDC's. The logic outputs of the CFD, LED High and LED Veto are stored in pattern units. Both the LED Low and the LED Veto information ware put in the multiplicity unit. This multiplicity unit counts the

[‡]For abbreviations see appendix A

number of neutral and charged hits per *TAPS*–block both in two levels: in this experiment ≥ 1 hit and ≥ 2 hits. These outputs are used in the trigger logic (section 3.1.5). The actual implementation of the *TAPS* electronics is shown in figure 3.6.

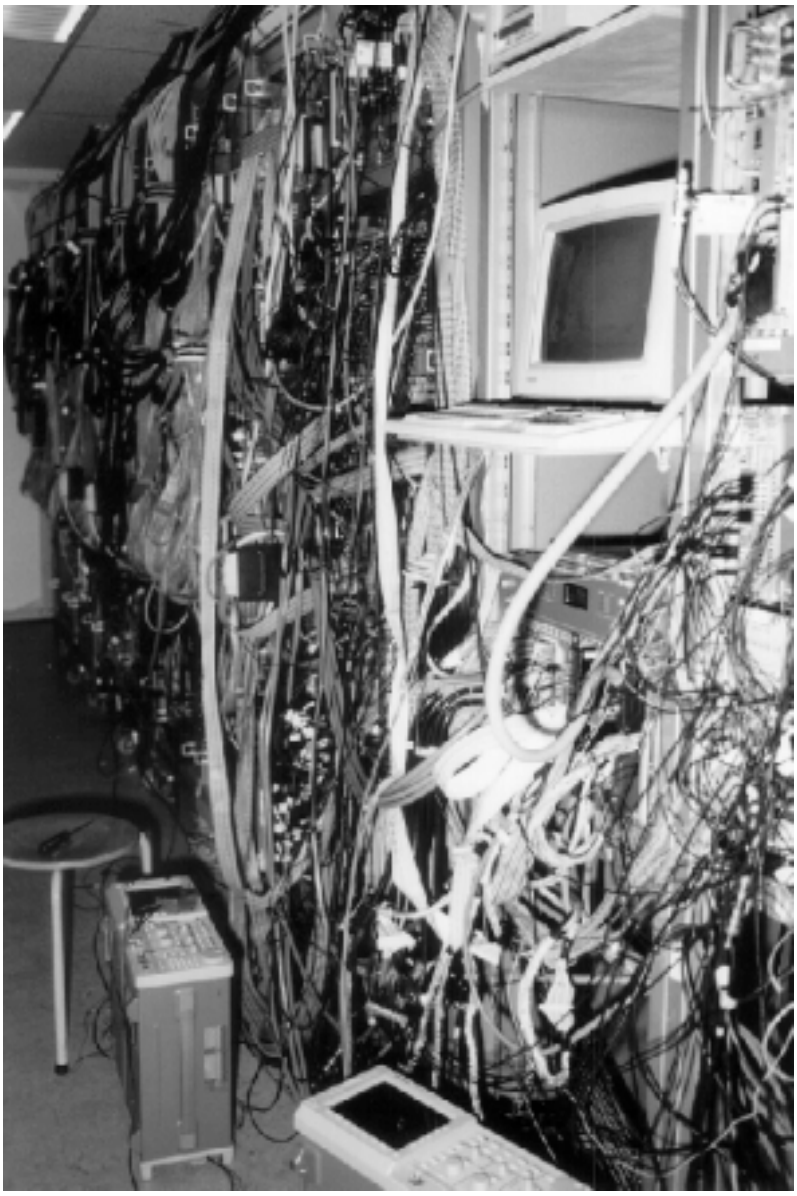

Figure 3.6: Photo of the *TAPS* electronics outside of the experimental hall.

3.1.4 SALAD

As can be seen in figure 3.1, the particles emitted forward were detected in *SALAD*. This Small–Angle Large–Acceptance Detector was especially designed for $pp\gamma$ studies at *KVI* [Kal98, Mes98].

3.1.4.1 The SALAD detector

In *SALAD*, forward emitted particles between 6° and 19° are detected over the whole azimuthal angular range. Two wire chambers (MWPC) determine the coordinates of the charged particles [Vol99]. The first one contains 3 planes (x, y and u (45°)) and has an active area of 380 $\times$ 380 mm^2. The u–plane allows to disentangle multiple hits. The second MWPC has 2 planes (x and y) and has an effective area of 840 $\times$ 840 mm^2. A hole in the middle of these wire chambers allows the beam to go through.

Behind the wire chambers are two layers of plastic scintillators. The first thick layer is used to measure the energy of the particles and the second thin layer is used to veto elastic events in experiments with high–energy protons. These protons punch through the thick layer reaching the thin layer. By vetoing these events, the event rates can be drastically reduced.

However, in case of the α + p experiment the veto could not be used for this purpose since also elastically scattered α particles and protons are stopped in the thick layer. The consequences are discussed in section 4.2.1. (The elastic events

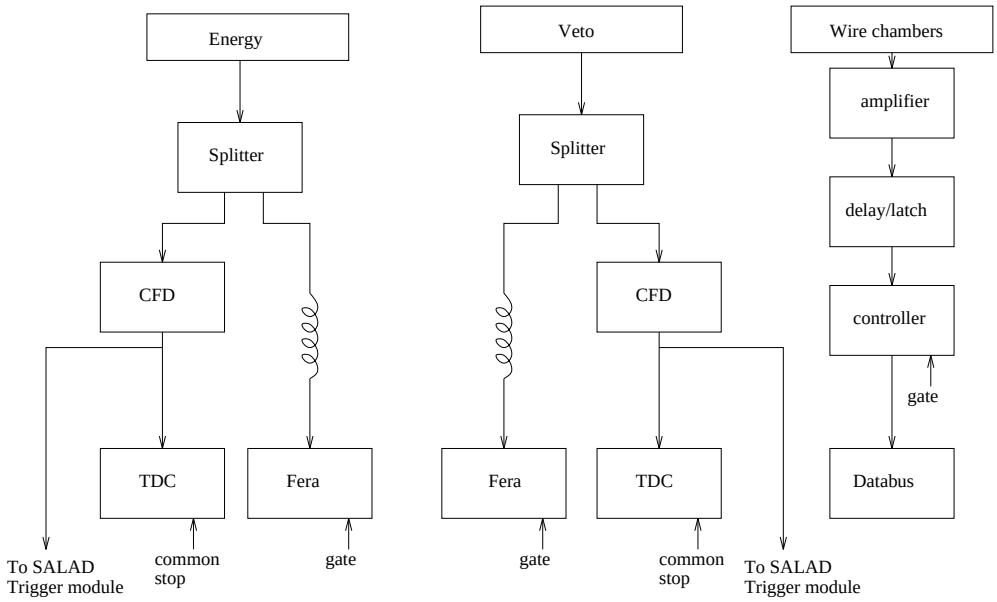

Figure 3.7: *SALAD* electronics scheme.

of this experiment have also been analyzed [Sei98]).

3.1.4.2 SALAD electronics

For *SALAD*, the time information and deposited energy information of both the energy and the veto scintillators are read out, as well as the hit wires of both wire chambers.

The *SALAD*–electronics scheme is shown in figure 3.7. The signals from the energy– and veto–scintillators follow the same trajectory. First, the signal is split into a time–branch and an energy–branch. The energy–branch is integrated in FERA's. The time–branch first passes a discriminator (CFD). Its output serves as an input for the *SALAD*–triggerbox (see section 3.1.3.2 and fig. 3.8) and is bussed to a TDC. The master trigger supplies the gates for the FERA's and TDC's.

The signals from the wire chambers are processed via amplifier/discriminator cards mounted on the chambers. In the delay/latch module, all channels are delayed in time and latched upon the controller receiving a gate from the master trigger. The controller performs the encoding of the hit wires. The digitized data are read out via a data bus.

3.1.5 Trigger Logic

The combined *TAPS* and *SALAD* trigger logic is shown in figure 3.8. Basically there are 3 trigger modules of which outputs are combined to make the master trigger. Up to 8 different triggers arrive at each trigger module and, depending on downscaling and dead time, making the Master Trigger. The individual trigger rates are also read out in scaler units: the raw, inhibited (deadtime corrected) as well as the output rates. The *TAPS* singles triggers (the CFD and LED OR's) as well as the beam current (not shown in the picture) serve as inputs for the *TAPS* trigger module. The beam current is not used to make a trigger, but its inhibited rate gives the effective integrated beam, which is used to calculate cross sections, i.e. it takes into account the elapsed time and deadtime:

$$\text{Integrated beam} = \text{beam current} \times \text{time} \times (1 - \text{deadtime fraction}). \qquad (3.1)$$

Using the outputs of the multiplicity units, the *TAPS* MLU's (Memory Lookup Units) make higher order triggers, such as 'Neutral low OR', 'pair'[¶] or 'quasi–neutral'[‖]. These outputs are used to validate the outcome of the *SALAD* trigger module [Sch99], which e.g. calculates the difference between the number of fired energy and veto detectors, which should be ≥ 2 for a ppγ candidate. The validation and the outcome of the *SALAD* trigger module together form the ppγ

[¶] two neutrals or one neutral and one charged in certain block combinations

[‖] per block a neutral LED Low or LED High

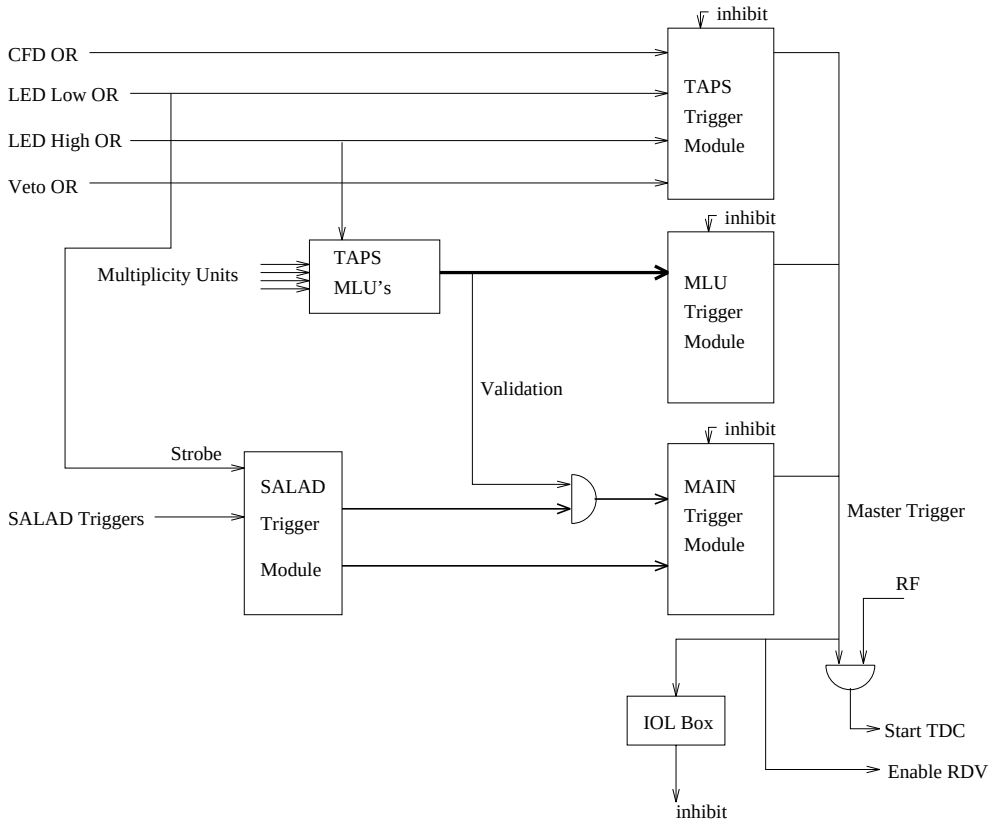

Figure 3.8: Combined *SALAD* and *TAPS* trigger scheme.

label	description	downscale
CFD	$E_{BaF_2} > 0.4$ MeV	2^{15}
LEDL	$E_{BaF_2} > 5$ MeV§	2^{9}
LEDH	$E_{BaF_2} > 10$ MeV	2^{6}
VETO	*TAPS* VETO OR	2^{10}
PPG	1 neutral in *TAPS* and 2 particles in *SALAD*	2^{0}
PG	1 neutral in *TAPS* and 1 particle in *SALAD*	2^{0}
PPG(TB)	like PPG, particles in top and bottom of *SALAD*	2^{0}
RF	downscaled RF	2^{8}

Table 3.2: Trigger selections. The upper part are the single triggers from the *TAPS* trigger box, the lower part from the main trigger box. (see figure 3.8)
§For the two most forward blocks, the threshold was set at 7 MeV.

(PPG) and pγ (PG) triggers (one photon in *TAPS* and two or one particles in *SALAD*, respectively). These are the main triggers in the α + p experiment, as listed in table 3.2. In the table, the upper triggers are the *TAPS* singles and the lower triggers the combined *TAPS* and *SALAD* triggers.

With a typical beam current of 0.4 pnA, the LED High trigger rate was 2.4 kHz and the PPG and PG trigger rates were 0.68 and 0.93 kHz, respectively. About 1 kHz of data was written to tape.

3.2 The carbon–fibre scattering chamber

The *Carbon–Fibre Scattering Chamber* was especially designed and constructed for use at the S-line (*Big-Bite Spectrometer* [Ber95]) and P-line (*SALAD*) at *KVI*, but it has recently also been used for *TAPS*–experiments at *GANIL*.

Carbon was chosen as a construction material of the scattering chamber because of its favourable properties as compared with iron, for example, which is more often used as a material for scattering chambers. This is shown in table 3.3, where the transmission probabilities are compared between a 4 mm carbon target and 3 mm thick iron, which are typical scattering chamber thicknesses. Also for neutrons and especially electrons and positrons the transmission is better for carbon than for iron.

More specifically for virtual bremsstrahlung experiments [Mes98] the use of carbon as a scattering chamber is important. In these experiments it is necessary to reduce the background of electron-positron pairs which are created by conversion of real photons in the walls of the scattering chamber. This background can be reduced by using a low "Z" material, since the cross section for conversion scales with Z^2. A 10 MeV photon has a conversion probability of 0.4 % when it passes through 4 mm thick carbon. For a 100 MeV photon this is 1.1 %. These same conversion probabilities are obtained when these photons pass through only 1.5 mm aluminium, or 0.35 mm iron. Carbon fibre is therefore a superior material for building a scattering chamber with a low conversion probability.

For experiments studying electron–positron pairs it is important to realize that when the real photons convert relatively far away from the target and near

P_{trans} through:	100 MeV photon	10 MeV neutron	10 MeV e^-	100 MeV e^-
4 mm Carbon	99 %	94 %	96 %	87 %
3 mm Iron	88 %	92 %	68 %	36 %

Table 3.3: Transmission probabilities of photons, neutrons and electrons through carbon and iron.

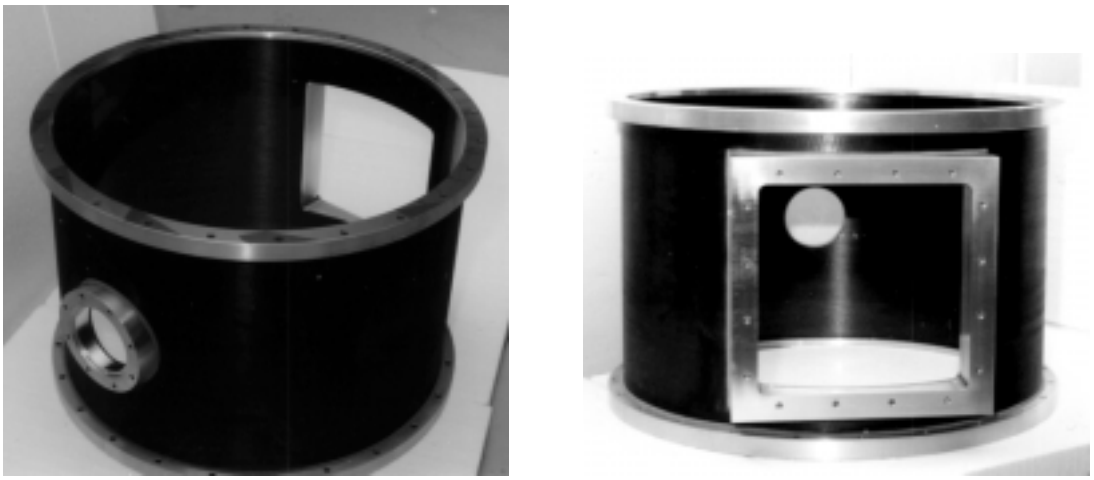

Figure 3.9: The *Carbon–Fibre Scattering Chamber*. The rectangular exit frame matches the opening angles of *SALAD* and the *Forward Wall*.

TAPS, the electron and the positron will hit the same detector or detectors that are close to each other. These events are less harmful since the apparent invariant mass will be small while the physics of interest is at large invariant mass. For large invariant masses, the electron–positron pairs will have mostly large opening angles. A chamber with a large diameter is therefore of great advantage.

The *Carbon–Fibre Scattering Chamber* is shown in figures 3.9 and 3.16. It has been designed by the drawing office of *KVI*. It has a diameter of 70 cm and a height of 50 cm. This height easily covers the opening angles of *TAPS* (fig. 3.16). The rectangular exit matches the opening angle of *SALAD* and the *Forward Wall*, which can also be put in front of the *Big-Bite Spectrometer*. In the case of usage at the *Big-Bite Spectrometer*, a bellow is placed at the entrance of the chamber, which allows the *Big-Bite Spectrometer* to rotate $\pm$ 4° around 0°. The structure of the 3.75 mm thick carbon walls are self supporting and is therefore uniform at all angles.

The strength of the chamber has been studied with a finite element calculation, performed by Visual Analysis [Vis]. It appeared that the construction was strong enough to withstand a pressure of 1.5 atm. Special attention was paid to stresses which occur in the carbon wall supporting the aluminium exit window. It appeared to be important to have very stiff lids on top and at the bottom of the chamber. A stiffness equivalent to a 5 cm thick aluminium lid is required, which should be bolted to the top and bottom ring. However, this procedure was not always followed for the top lid, with no apparent harm.

The chamber was constructed by Stesalit [Ste]. To minimize outgassing of the carbon walls, first a 100 μm thick mylar foil was wrapped around the mandrel

used for the chamber. Then the carbon was wound. The entrance and the exit frames are glued to the carbon. An extra layer of epoxy was put at the frame boundaries to guarantee vacuum tightness.

During the experiments with *SALAD*, a vacuum of 10^{-4} mbar could be reached within ~ 3 to 4 hours. To reach a vacuum of $6.3{\cdot}10^{-6}$ mbar (best value), a much longer period was needed. However, the LH_2 target acted as a cryopump, and a vacuum of $3{\cdot}10^{-6}$ mbar could be reached within minutes after starting with cooling. The best measured vacuum was $6.6{\cdot}10^{-7}$ mbar.

3.3 Forward Wall

The *Forward Wall* has not been a part of the setup of the $\alpha + \mathrm{p}$ experiment. However, it is described here since it is one of the general experimental facilities for the *KVI* in which the author was particularly involved.

In typical heavy–ion reactions many light charged fragments can be produced. These fragments can have different origins like pre-equilibrium emission in the early stage of the reaction, evaporation from the projectile-like fragment (PLF) or target-like fragment (TLF). While the fragments from the latter process will be more or less isotropically emitted, those from the first two will be predominantly focussed to small angles, in particular those from the PLF.

If all light charged particles (LCPs) can be detected in coincidence with the PLF, the atomic number of the PPLF (primary PLF) can be reconstructed [Pol95]. This 'reconstructed' fragment in coincidence with the detection of hard photons has been used, for example, to investigate the dissipation mechanisms in peripheral nucleus–nucleus collisions at intermediate energies [Pol96, Pol96a]. Alternatively, the LCP multiplicity can be used as a measure of the impact parameter [Mar94, Mar94a, Mar95a, Mar95b].

3.3.1 Extension of the Forward Wall

The *KVI–Forward Wall* is designed to detect fast LCP's. It has been used in various different setups at *KVI* and *GANIL* experiments [Lee92, Mar94, Mar94a, Pol95, Mar95a, Mar95b, Pol96a]. For the use of the *Forward Wall* during the *TAPS* campaign at *KVI* of 1996–1997 and at *GANIL* in 1998, it has been extended with extra detectors to increase the granularity and to allow for higher count rates per solid angle.

3.3.1.1 Phoswiches

The basic ingredient for the detection of the LCP's are the phoswich detectors [Lee92a]. They consist of a 1 mm thick so-called 'fast' plastic (τ=2.4 ns), NE102A, and 50 mm thick 'slow' plastic (τ=320 ns), NE115 (fig. 3.10), which are

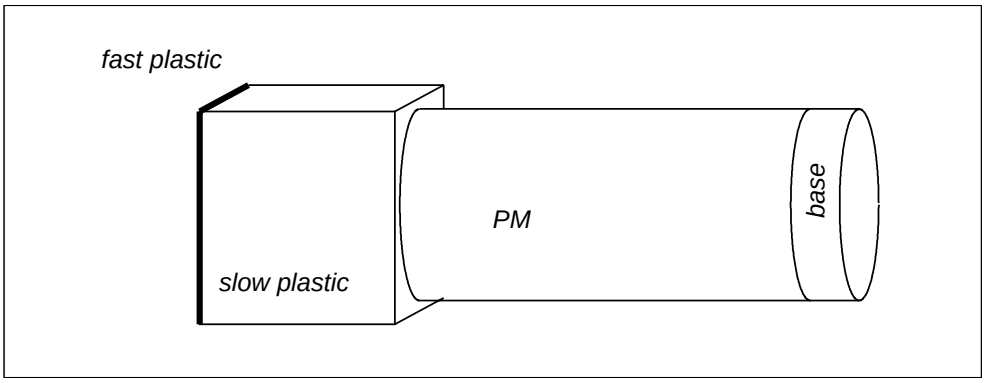

Figure 3.10: Schematic phoswich detector with at the left side both scintillating plastics which are glued to the photomultiplier (PM).

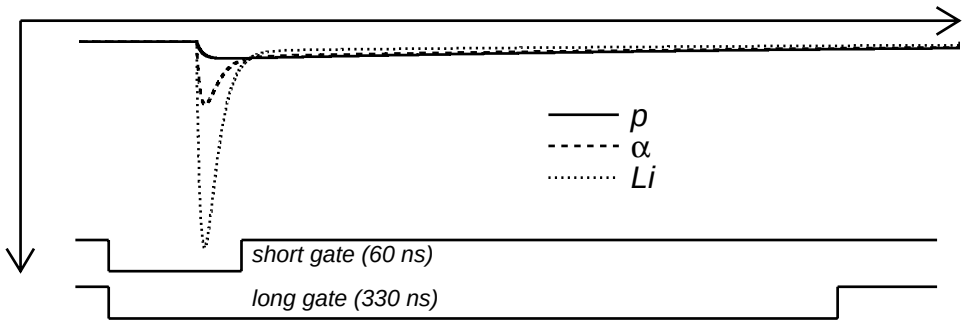

Figure 3.11: Pulse shapes for different particles in the phoswich detector.

heatpressed together [Kol86, Lid87]. This heatpressing is important for a good coupling, without a dead layer, between the two plastics.

A photomultiplier is glued to the backside of the phoswich with a two–component epoxy or a silicon glue. A photomultiplier base distributes the high voltage over the dynodes of the photomultiplier.

The light output is the sum of the light outputs of both plastics of the phoswich (fig. 3.11). By integrating this light output over two different time intervals (gates), it is possible to obtain the energies deposited in the thin (ΔE) and the thick plastic (E), respectively. On basis of the correlation between the energy loss ΔE (short gate) and the total energy E (long gate) one can distinguish between the different light charged particles and identify them. In a ΔE–E scatter plot, the different particles can be recognized as separate bands (fig. 3.18).

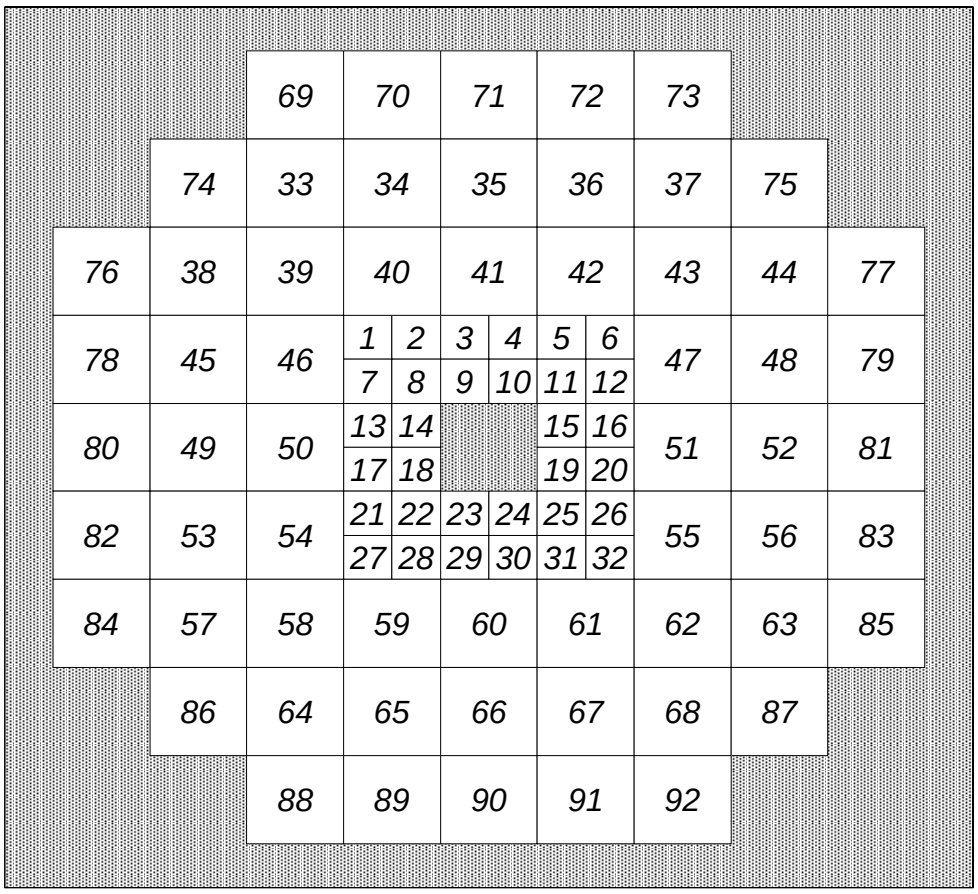

Figure 3.12: Schematic view of the *Forward Wall*, showing the used numbering of the individual detectors.

3.3.1.2 Design

In figure 3.12 the extended *Forward Wall* is drawn schematically. In total it consists of 92 phoswich detectors. At the most forward angles, where the count rates are highest, 32 small phoswiches are positioned. They each cover a surface of 32.5×32.5 mm^2 and have a 10-stage photomultiplier (type XP2972). Around these most central modules, 60 large phoswiches are positioned, each covering a surface of 65×65 mm^2. The outer ring (numbers 69–92) utilizes the older detectors, which have a 12-stage photomultiplier (type 9814B). Numbers 33–68 are the new detectors. They have an 8-stage photomultiplier (type XP2282B) and a specially designed active base (VD182K/B01) [Hui95]. It operates at a high quiescent current of about 0.7 mA in order to keep the amplification of the photomultipliers stable, also at high countrates.

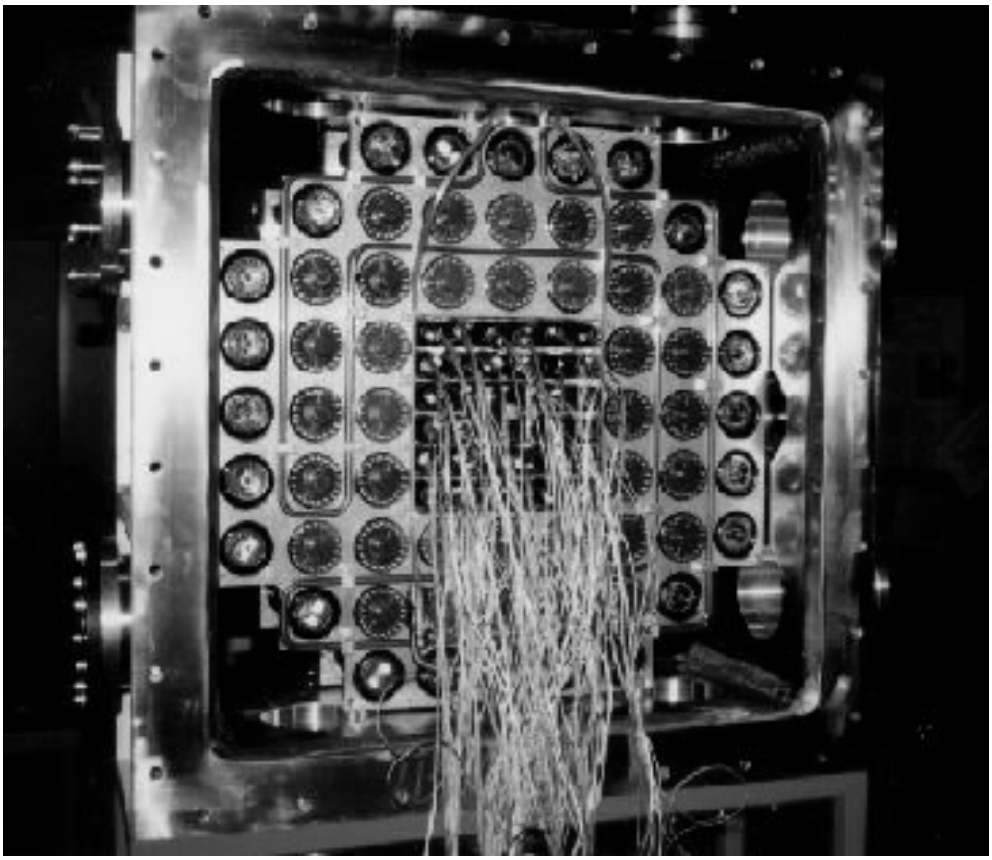

Figure 3.13: Backside of a partially filled *Forward Wall*. The small Cu pipe providing the cooling of the detectors can be seen.

The *Forward Wall* covers an angular range of $2.5° < \theta < 25.5°$ at a full ϕ range. The hole in the middle allows the beam and the PLF's to pass through. A specially designed double–frame construction keeps the individual detectors at their position (fig. 3.13). The backside frame needs cooling to dissipate the heat generated by the PM-bases, in order to allow the *Forward Wall* to be used in vacuum. This cooling is realized by liquid alcohol at -40°C which flows through a small Cu pipe, attached to the backward frame. Several probes allow to check on the temperatures.

The whole *Forward Wall* construction is placed in an aluminium box, with flanges for cable feedthroughs, cooling pipes and pumping. This frame allows for building up and testing the *Forward Wall* 'offline' and for transport purposes. It has been designed especially to be operated with the KVI *Big-Bite Spectrometer* [Ber95] for coincidence experiments. It can be attached to the *Carbon–Fibre Scattering Chamber* (section 3.2) as well. The experiment described in section

3.3.2, took place in the P–line (not with the *Big-Bite Spectrometer*).

Despite all materials used inside the *Forward Wall* a vacuum of about $2 \cdot 10^{-5}$ mbar could be reached within the vacuum area of the *Carbon–Fibre Scattering Chamber* and *Forward Wall*.

3.3.1.3 Electronics

In figure 3.14 a block diagram of the electronics scheme of the *Forward Wall* is shown. Signals from the photomultiplier are split in an active splitter into a so–called *time-branch* and an *energy-branch*.

In the time-branch the signal is converted into an equivalent charge output for all channels, using the Le Croy 3420 Constant–Fraction Discriminator (CFD). The signal starts the output of the CFD and a veto terminates the output. The veto arrives at the same time for all detectors and is related to the RF of the cyclotron. The output of the CFD is first delayed and then integrated in a

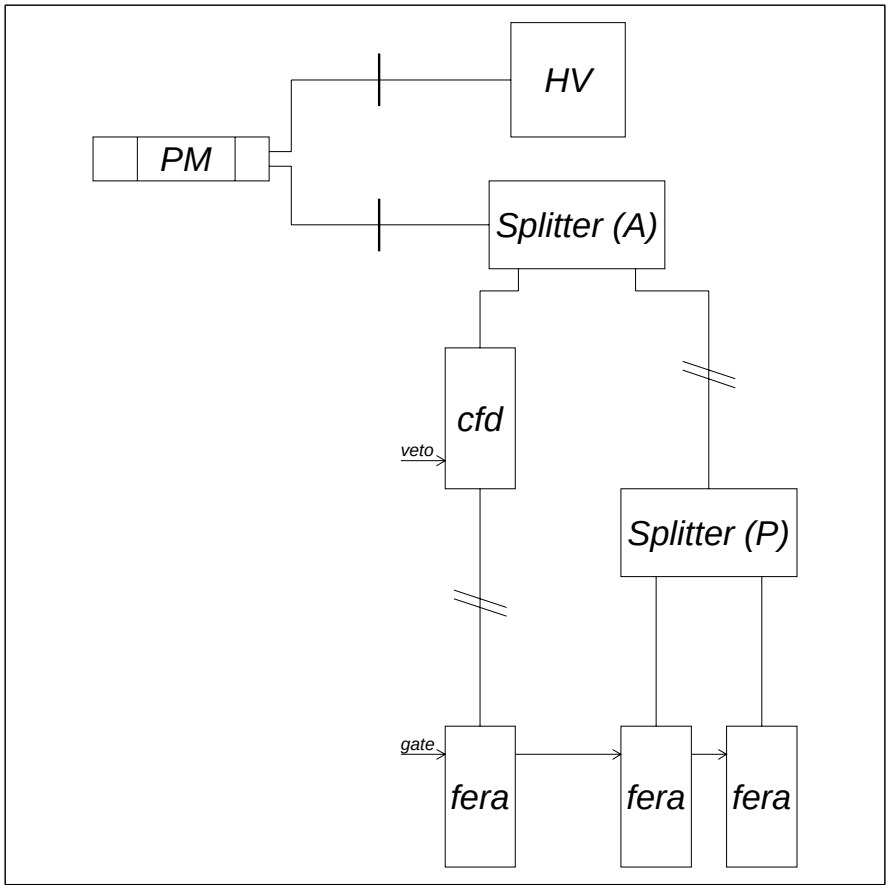

Figure 3.14: *Forward–Wall* electronics scheme.

Fast Encoding and Readout ADC (FERA, LeCroy 4300B). The later the particle arrives at the *Forward Wall*, the smaller the output.

As mentioned in section 3.3.1.1, the energy–branch has to be integrated twice: within a short–time gate and a long–time gate to obtain the pulse shape information for the identification of the particles. To this end, the signal of the energy branch, after being delayed, is split into two signals by a passive splitter. The integration is done by FERA's. The *TAPS* main trigger (fig. 3.8) generates the gates, which are derived from the RF signal. This eliminates the jitter as discussed by Leegte [Lee92]. The gates were 95 ns for the short gate and 300 ns for the long one.

Readout was done via the fast ECL output ports of the FERA to the FERA Driver (LeCroy 4301). From there the data were transferred to a VME Dual–

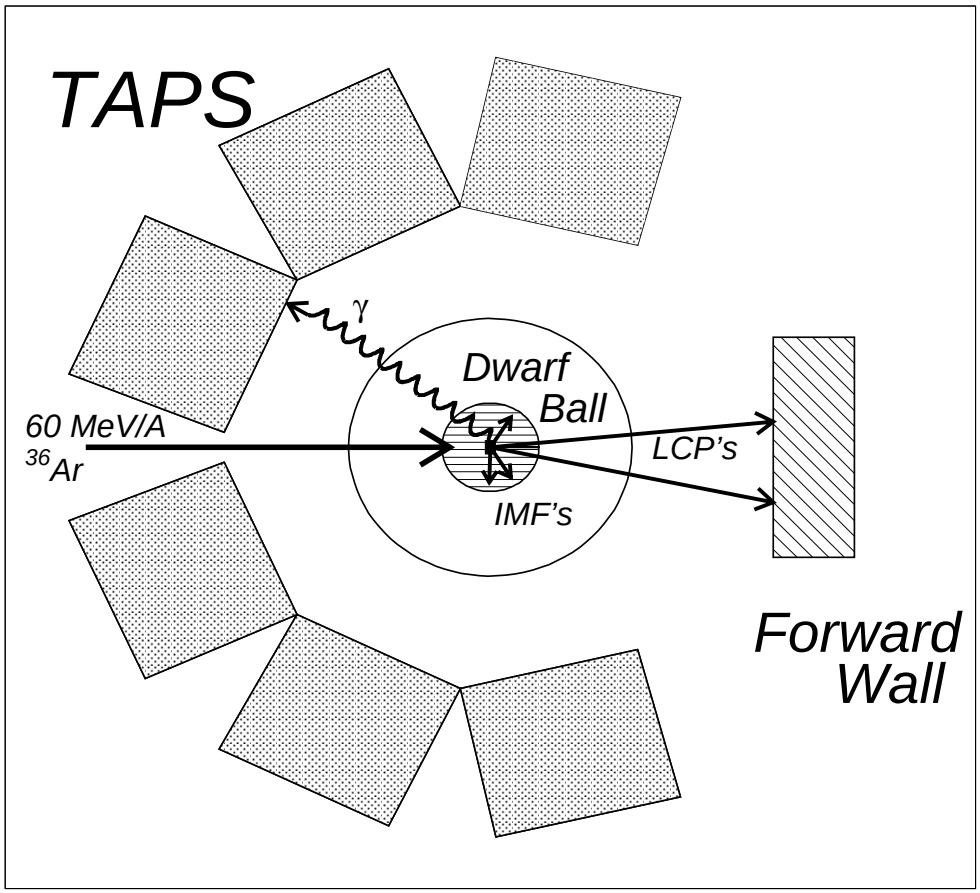

Figure 3.15: Setup of *TAPS*, the *Forward Wall* and the *Dwarf Ball* in the ^{36}Ar + Au experiment.

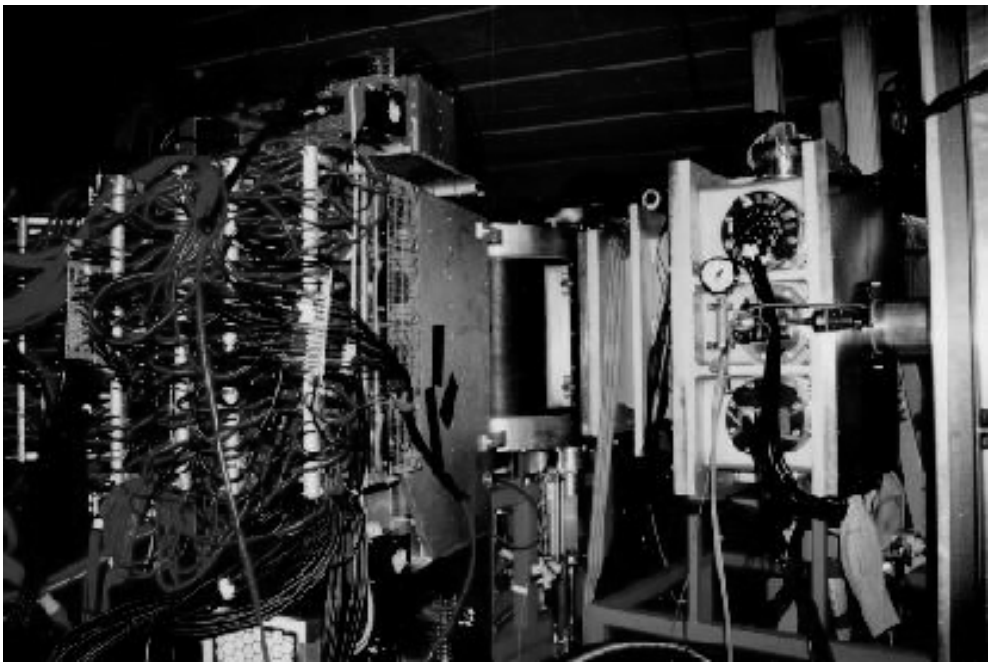

Figure 3.16: Photo of the setup for the ^{36}Ar + Au experiment showing the *Carbon–Fibre Scattering Chamber*, the back of one of the *TAPS* blocks and at the right side the chamber housing the *Forward–Wall* detectors.

Port Memory (LeCroy 1190). In the experiment described in section 3.3.2, the *Forward Wall* data are combined by a processor with the *TAPS* and *Dwarf Ball* data into one event.

3.3.2 Performance at experiment

The first experiments with the extended *Forward Wall* were made at the end of 1997 when the heavy–ion experiments with *TAPS* were performed at *KVI*. In the case of the 60 MeV/u ^{36}Ar+^{nat}Au** experiment, the aim was to study the properties of hot and dense nuclear matter, like temperature, density and size. To this extent, hard and thermal photons were measured in coincidence with light charged particles and intermediate–mass fragments (IMF), the latter allowing to select the most dissipative reactions.

**KVI experiment R2.

3.3.2.1 Setup

The photons were detected in *TAPS* (3.1.3) which was positioned in 6 blocks around the scattering chamber (fig. 3.15 and 3.16). At forward angles, the *Forward Wall* was used to detect the light charged particles. Within the scattering chamber, close around the target, the *Dwarf Ball* [Str90] was used as an intermediate–mass–fragment detector.

In figure 3.16 the *Forward Wall* in its vacuumbox can be seen on the right–hand side. A part of the *Carbon–Fibre Scattering Chamber* is visible between one of the *TAPS* blocks on the left–hand side and the *Forward–Wall* chamber. The beam is coming from the left. The *Dwarf Ball* is inside the *Carbon–Fibre Scattering Chamber*.

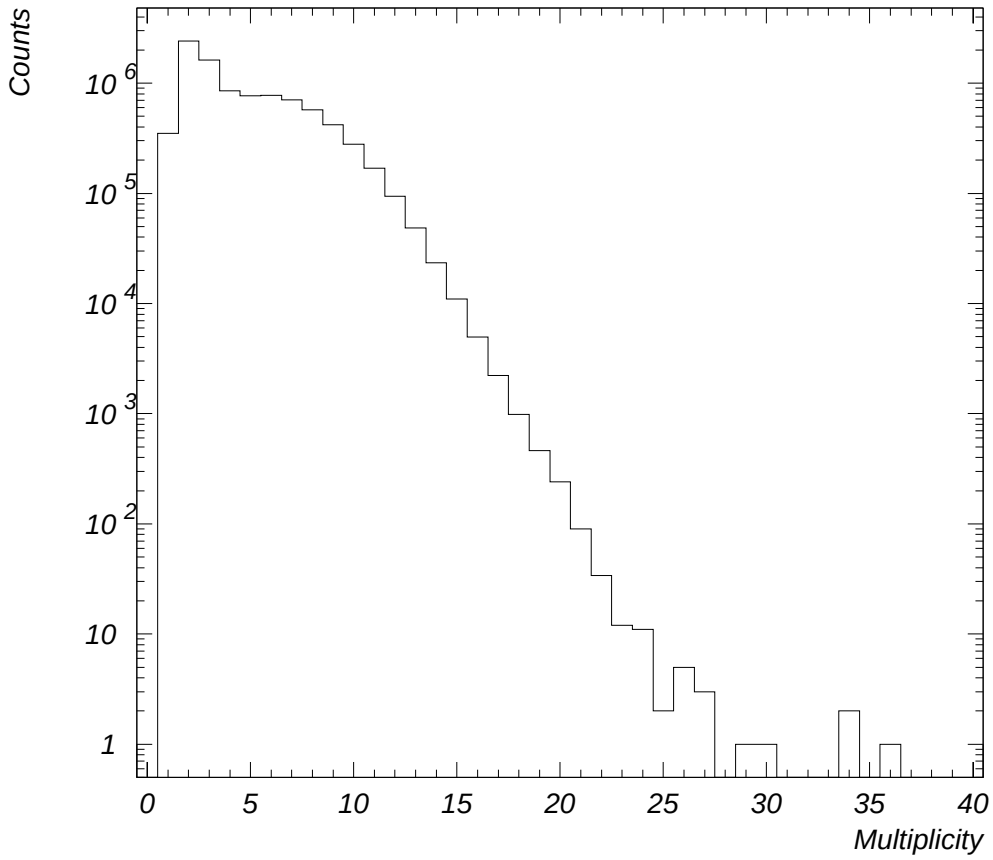

Figure 3.17: *Forward–Wall* multiplicity distribution in the ^{36}Ar + Au experiment at 60 MeV/u.

3.3.2.2 Results

In the experiment, an ^{36}Ar beam of 60 MeV/u delivered by *AGOR* impinged on a 7.5 mg/cm^2 Au target. The beam current was about 3 enA and the *Forward–Wall* detectors handled a count rate up to 600 kHz. The total count rate being in the order of 4.5 MHz.

The *Forward–Wall* multiplicity distribution is plotted in figure 3.17. Since the experiment mainly triggered on central events, high multiplicities are reached. In the case shown, pileup from random coincident events was about 4 %.

A typical ΔE–E spectrum from this experiment is shown in figure 3.18. The isotope identification of hydrogen: protons, deuterons and tritons can be seen in the inset of figure 3.18. Not only the LCPs could be identified with the *Forward Wall*, but also the IMF's emitted in the forward direction. As seen in the figure particles could be observed and identified up to nitrogen.

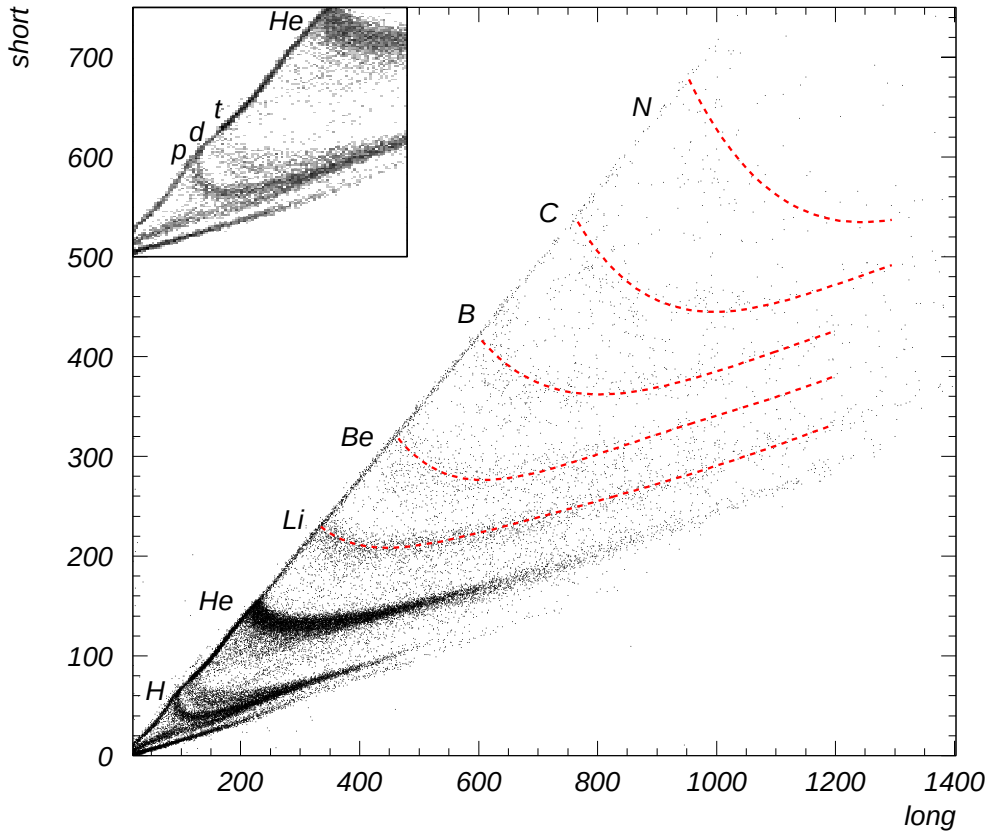

Figure 3.18: *Forward–Wall* particle identification. The inlet shows the isotope separation of hydrogen.

Part of the *Forward Wall* was covered by a 100 μm thick Ni absorber to shield against elastically scattered particles and δ–rays. This increases the thresholds of detected particles. All particles have to punch through the first 1 mm of plastic to be identified, since particles which are stopped in the fast plastic will end up on the '$\Delta E = C \cdot E$' line and can therefore not be identified (see fig 3.18). When the particles also punch through the 50 mm of slow plastic, the detected energy is not anymore equal to the total energy of that particle, but decreases with increasing particle energy. Consequently, the different particles are not distinguishable anymore. However, by using time–of–flight in addition, the particles can still be identified. The threshold and maximum energy values are put in table 3.4, with and without absorber.

In figure 3.19 a time spectrum of the *Forward Wall* is shown from the 50 MeV/u Xe+Sn experiment[††] at *GANIL* (1998). No particle or energy selection is made here, resulting in a time resolution of 2.8 ns (FWHM).

Particle	Threshold (MeV/u)		Max. energy (MeV/u)
	no absorber	100 μm Ni	
p	9.1	11.5	81
d	6.2	7.8	56
t	4.9	6.1	44
He	9.1	11.5	81
Li	10.5	13.2	93
Be	12.6	15.9	112
B	14.4	18.1	128
C	16.8	21.2	150
N	18.1	23.0	165

Table 3.4: Punch–through energies.

[††]GANIL experiment E300

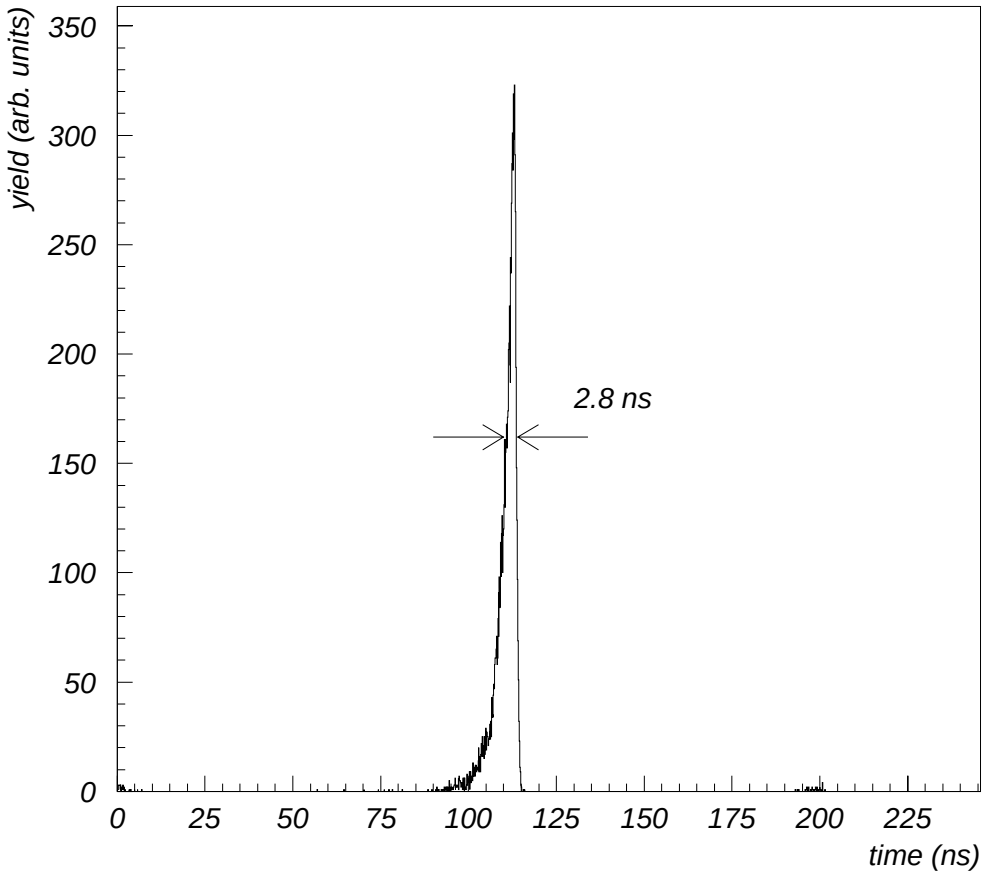

Figure 3.19: *Forward–Wall* calibrated time spectrum.